Direct Baseband I-Q Regeneration Method for Five-Port Receivers Improving DC-offset and Second-Order Intermodulation Distortion Rejection

C. de la Morena-Álvarez-Palencia, K. Mabrouk, B. Huyart, A. Mbaye, M. Burgos-García

***Abstract*—Six/Five-port architecture has advantages compared to conventional receiver architectures, especially for high frequencies and high data rate applications. However, it requires two/one additional baseband outputs and a calibration process to recover the original signal. While this problem is resolved in conventional six-port configurations, a solution is needed for five-port architectures. We propose an I/Q regeneration method based on the use of a simple analog circuit, eliminating one baseband output. The structure of this circuit derives from a mathematical formulation, which is presented in this paper. The validity of the method has been experimentally proved in a five-port receiver prototype. In addition, its capacity to reduce the DC-offset and second-order intermodulation distortion (IMD2) has been demonstrated.**

***Index Terms*—Five-port, five-port calibration, receivers, reconfigurable architectures, six-port, zero-IF.**

I. Introduction

Superheterodyne architecture has been the classical radiofrequency (RF) architecture in radiocommunications, due to its selectivity and sensitivity characteristics. However, superheterodyne transceivers are complex, and expensive, and they require a large number of external components. On the contrary, zero-IF and low-IF architectures have important competitive advantages, such as simplicity, compact size, flexibility, reconfigurability and high level of integration [1]-[3]. Comparing with the superheterodyne architecture, a frequency conversion stage is eliminated, including the image-reject filter. In addition, principal operations are carried out in baseband, where low-cost integrated devices can be used. Nevertheless, these architectures have some limitations. In the case of zero-IF receivers, these limitations include DC-offset, 1/f noise, and second-order intermodulation distortion (IMD2). Regarding the low-IF configuration, the image frequency continues being the main problem. Moreover, the trend towards high data rate services will require very large bandwidths, which become possible at high frequencies. However, I-Q mod/demodulators need a nearly perfect 90º phase shift between their I-Q paths, which cannot be guaranteed over a very broad bandwidth. Therefore, the use of zero-IF and low-IF architectures is limited by these devices.

An alternative to the classical zero-IF and low-IF architectures is the six(five)-port architecture [4]-[5], either with the use of a six-port circuit [6], a five-port circuit [7] or a three-phase circuit [8]. The block diagrams of a five-port receiver using, respectively, a five-port circuit and a three-phase circuit are shown in Fig. 1 (a) and Fig. 1 (b). For a six-port receiver, the structure is like that shown in Fig. 1 (a), but with one additional output port. The main characteristic of the six(five)-port architecture is its extremely large bandwidth, which involves multi-band and multi-mode capabilities [6],[9]. Six(five)-port networks can operate at very high frequencies, being a serious alternative for millimeter-wave frequencies and high data rate applications [10]-[13]. Nevertheless, as it happens with the conventional zero-IF architecture, DC-offset, 1/f noise and IMD2 are its drawbacks. In addition, a calibration process is required to recover the original I-Q signals, and more baseband outputs are needed (hence more low-pass filters, video amplifiers, analog to digital converters, etc.).

The reduction to four-port receivers has been reported in the literature [14]-[15]. However, four-port receivers are limited to applications with low input signal levels. Otherwise, a complex calibration procedure is required to recover I-Q signals without distortion, since the relation between I-Q and output signals is nonlinear [14]. The typical six-port topology admits analog I/Q regeneration by means of a simple circuit, eliminating two baseband branches and the calibration process [10]-[12]. This is possible due to the particular characteristics

Manuscript received September 28, 2011. This work was supported in part by the Institut Telecom, TELECOM ParisTech, in the framework of "future et rupture DEMODU program", and by the grant "IX Convocatoria de Ayudas del Consejo Social, Universidad Politécnica de Madrid".

C. de la Morena Álvarez-Palencia, and M. Burgos-García are with the Grupo de Microondas y Radar, Departamento de Señales, Sistemas y Radiocomunicaciones, Universidad Politécnica de Madrid, 28040 Madrid, Spain (e-mail: cmorena@gmr.ssr.upm.es, mateo@grm.ssr.upm.es).

B. Huyart, and A. Mbaye are with the Département Communications et Electronique, Institut Telecom, TELECOM ParisTech, 75016 Paris, France (e-mail: huyart@telecom-paristech.fr, ambaye@telecom-paristech.fr).

K. Mabrouk is with ESIGETEL (Ecole en Informatique et Télmecommunications), (e-mail: kais.mabrouk@esigetel.fr).

of this six-port topology: the local oscillator (LO) and RF signals are combined with equal amplitudes, and relative

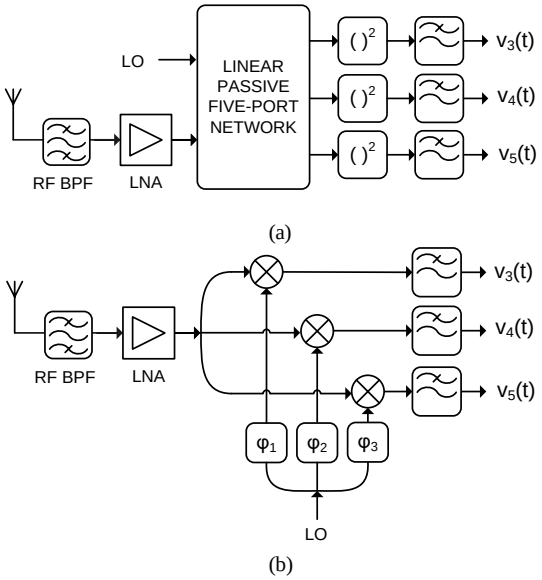

Fig. 1. Five-port receiver (a) Based on a five-port circuit, (b) Based on a three-phase circuit.

phase shifts of 0, π/2, -π/2, and π rad. However, the habitual procedure in five-port receivers is to digitalize the three output signals and apply a calibration algorithm [7]-[8]. Some first approaches of analog I-Q regeneration in five-port receivers used the above mentioned six-port topology with one port reduction [17]. From these particular five-port parameters, a formulation is derived and an analog circuit is proposed to recover the original I/Q components. However, the particular conditions from which the analog circuit is derived in [17] cannot be extended to a general five-port network. For example, the design criterion of an optimal five-port network imposes relative phase shifts of 0º, 120º, and -120º. In this paper, we propose a new, general, and simple method to recover the original I/Q signals in five-port architectures, without using any calibration process. It is based on the use of an analog I/Q regeneration circuit [16], whose structure is derived from a mathematical formulation, which is valid for any kind of five-port topology fulfilling simple necessary conditions. In fact, it will be demonstrated that the work presented in [17] responds to a particular case of the proposed method. The analog I/Q regeneration circuit can be easily integrated without adding complexity to the original circuit. The proposed method solves the above-mentioned six(five)-port architecture drawbacks, as it eliminates one baseband output and the calibration algorithm without any reduction in the operating frequency band. Moreover, the method allows not only to recover the original I-Q signals, but also to reduce the DC-offset and IMD2. Consequently, the dynamic range can be extended due to the lower output voltages, as a consequence of the DC-offset and IMD2 reduction.

II. Fundamentals of the Five-Port Technique

The principle of operation of the five-port receiver is based on the measurement of three independent powers, when the LO and RF signals are introduced into the remaining two ports. The original I/Q components can be regenerated from these three power observations and some calibration constants, depending on system response [4]-[5]. The typical five-port receiver configuration is presented in Fig. 1 (a). It is composed of a linear passive five-port circuit, where the RF and LO signals are combined using different relative phases. A square law device and a low-pass filter are located at each output. A variation to the typical five-port configuration is the three-phase circuit [8], shown in Fig. 1 (b). The difference is that the three-phase receiver uses mixers instead of power detectors. Nevertheless, both architectures are based on the same operation principle, which is described in detail in [7],[18]. The output signal at port *i*, $v_i(t)$, after the diode detection and ideal low-pass filtering, can be expressed as

$$v_i(t) = \frac{K_{2i}}{2} A_i^2 V_{LO}^2 + \frac{K_{2i}}{2} B_i^2 \left[I^2(t) + Q^2(t)\right] + \\ + K_{2i} V_{LO} A_i B_i \cos(\varphi_i - \psi_i) I(t) + \\ + K_{2i} V_{LO} A_i B_i \sin(\varphi_i - \psi_i) Q(t) \quad , i=\{3,4,5\} \qquad (1)$$

where I and Q are the in-phase and quadrature-phase modulating signals, and V_{LO} is the LO amplitude. A_i and φ_i are, respectively, the attenuation and phase shift of the five-port circuit from the LO port at the frequency $f=f_{RF}$ (frequency of the modulated signal)=f_{LO} (LO frequency), while B_i and ψ_i correspond to the RF port. K_{2i} is the second order coefficient of the diode transfer characteristic at port *i*. The output signals $v_i(t)$ are composed of the self-mixing of the LO, which is a DC component, the self-mixing of the modulated useful signal, and the wanted signal components. The self-mixing of the modulated signal comprises a dc component, dc_i, and a time variant component, $n(t)$, that is:

$$\frac{K_{2i}}{2} B_i^2 \left[I^2(t) + Q^2(t)\right] = dc_i + R_i n(t), \qquad (2)$$

with $R_i = \frac{K_{2i}}{2} B_i^2$.

Then, (1) can be rewritten as follows:

$$v_i(t) = V_{dc,i} + R_i n(t) + S_i \cos\phi_i I(t) + S_i \sin\phi_i Q(t), \qquad (3)$$

where:

$$V_{dc,i} = \frac{K_{2i}}{2} A_i^2 V_{LO}^2 + dc_i, \qquad (4)$$

$$S_i = K_{2i} V_{LO} A_i B_i \text{ , and} \qquad (5)$$

$$\phi_i = \varphi_i - \psi_i . \qquad (6)$$

For the three output signals, the following system of equations can be written:

$$\begin{bmatrix} v_3(t) \\ v_4(t) \\ v_5(t) \end{bmatrix} = \begin{bmatrix} R_3 & S_3\cos\phi_3 & S_3\sin\phi_3 \\ R_4 & S_4\cos\phi_4 & S_4\sin\phi_4 \\ R_5 & S_5\cos\phi_5 & S_5\sin\phi_5 \end{bmatrix} \cdot \begin{bmatrix} n(t) \\ I(t) \\ Q(t) \end{bmatrix} + \begin{bmatrix} V_{dc,3} \\ V_{dc,4} \\ V_{dc,5} \end{bmatrix}. \quad (7)$$

The term $V_{dc,i}$ represents the DC-offset of the output voltages, which can be removed by subtracting the average: $\hat{v}_i(t) = v_i(t) - V_{dc,i}$. In that case, the previous system can be solved by means of a matrix inversion, leading to the well known five-port demodulation equations

$$I(t) = r_I\hat{v}_3(t) + s_I\hat{v}_4(t) + t_I\hat{v}_5(t) \quad (8)$$

$$Q(t) = r_Q\hat{v}_3(t) + s_Q\hat{v}_4(t) + t_Q\hat{v}_5(t) \quad (9)$$

where r_I, s_I, t_I, r_Q, s_Q, and t_Q are the so-called calibration constants. Therefore, a system calibration is required to calculate these calibration constants, and to recover the I/Q components of the original signal.

III. Description of the I/Q Regeneration Method

The present I/Q regeneration method is based on the assumption that there is a symmetry axis in port 4 [16]. That means that the amplitudes of the output signals in ports 3 and 5 have to be equal, and their phase shifts with respect to the signal in port 4 have to be complementary. Therefore, the next two symmetry conditions have to be fulfilled:

(I) Amplitude symmetry condition:

$$A_3 = A_5\ , B_3 = B_5\ , K_{23} = K_{25} \quad (10)$$

(II) Phase symmetry condition:

$$\phi_3 = C_0 + \gamma\ , \phi_4 = C_0\ , \phi_5 = C_0 - \gamma \quad (11)$$

To simplify the expressions, we will choose C_0 = 0, which will only cause a rotation of the constellation. This rotation can be easily compensated by an equalization process. Under amplitude and phase symmetry conditions, (7) reduces to

$$\begin{bmatrix} v_3(t) \\ v_4(t) \\ v_5(t) \end{bmatrix} = \begin{bmatrix} R_3 & S_3\cos\gamma & S_3\sin\gamma \\ R_4 & S_4 & 0 \\ R_3 & S_3\cos\gamma & -S_3\sin\gamma \end{bmatrix} \cdot \begin{bmatrix} n(t) \\ I(t) \\ Q(t) \end{bmatrix} + \begin{bmatrix} V_{dc,3} \\ V_{dc,4} \\ V_{dc,3} \end{bmatrix}. \quad (12)$$

Consequently, the calibration constants result in:

$$r'_I = -\frac{1}{2S_3}\frac{\beta}{\alpha - \beta\cos(\gamma)} \quad (13)$$

$$s'_I = -\frac{1}{S_3}\frac{1}{\alpha - \beta\cos(\gamma)} \quad (14)$$

$$t'_I = r'_I \quad (15)$$

$$r'_Q = -\frac{1}{2S_3}\frac{1}{\sin(\gamma)} \quad (16)$$

$$s'_Q = 0 \quad (17)$$

$$t'_Q = -r'_Q \quad (18)$$

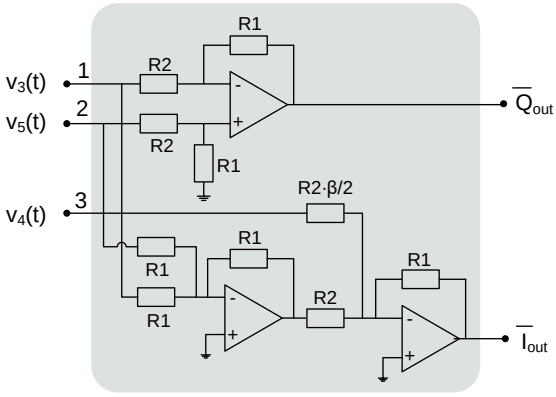

Fig. 2. Structure of the analog I/Q regeneration circuit

with: $\beta = \frac{R_4}{R_3}$,and $\alpha = \frac{S_4}{S_3}$.

Substituting (13)-(18) into (8)-(9), we obtain

$$I(t) = \mu_I[-v_3(t) + \frac{2}{\beta}v_4(t) - v_5(t)] + \mu_I V_{dcI} \quad (19)$$

$$Q(t) = \mu_Q[v_3(t) - v_5(t)] - \mu_Q V_{dcQ} \quad (20)$$

being:

$$\mu_I = \frac{1}{2S_3}\frac{\beta}{\alpha - \beta\cos(\gamma)} \quad (21)$$

$$\mu_Q = \frac{1}{2S_3}\frac{1}{\sin(\gamma)} = \frac{\beta\sin(\gamma)}{\alpha - \beta\cos(\gamma)} \cdot \mu_I \quad (22)$$

$$V_{dcI} = -V_{dc,3} + \frac{2}{\beta}V_{dc,4} - V_{dc,5} \quad (23)$$

$$V_{dcQ} = V_{dc,3} - V_{dc,5} = 0\,. \quad (24)$$

Note that the amplitude symmetry condition (10) involves that the DC component in the Q-path, V_{dcQ}, is null, since $V_{dc,3}$ is equal to $V_{dc,5}$. The two expressions given by (19) and (20) can be easily performed by a low-cost operational-amplifier-based circuit, as that shown in Fig. 2. The output voltages $v_3(t)$, $v_5(t)$, and $v_4(t)$, are injected into the input ports 1, 2 and 3, respectively. The first operational amplifier performs the subtraction of $v_3(t)$ and $v_5(t)$. The other two amplifiers perform the sum of $v_5(t)$ and $v_3(t)$, and the subtraction of twice the voltage $v_4(t)$ divided by β. This provides the $I_{out}(t)$ and $Q_{out}(t)$ signals, which are equal to the original I/Q signals, excepting for the factors $1/\mu_I$ and $1/\mu_Q$:

$$I_{out}(t) = -v_3(t) + \frac{2}{\beta}v_4(t) - v_5(t) = \frac{I(t)}{\mu_I} - V_{dcI}\,, \quad (25)$$

$$Q_{out}(t) = v_3(t) - v_5(t) = \frac{Q(t)}{\mu_Q}\,. \quad (26)$$

The expression of the I_{out}/Q_{out} signals regenerated from the proposed technique can be obtained by substituting the values of the three output signals given by (3) into (25)-(26):

$$\begin{bmatrix} I_{out}(t) \\ Q_{out}(t) \end{bmatrix} = \begin{bmatrix} \vec{a}_I \\ \vec{a}_Q \end{bmatrix} \cdot \begin{bmatrix} I(t) \\ Q(t) \end{bmatrix} + \begin{bmatrix} R_I \\ R_Q \end{bmatrix} \cdot n(t) + \begin{bmatrix} V_{dcI} \\ V_{dcQ} \end{bmatrix} \quad (27)$$

where

$$\vec{a}_I = \left(-S_3\cos\phi_3 + \frac{2}{\beta}S_4\cos\phi_4 - S_5\cos\phi_5 \ , \ S_3\cos\phi_3 - S_5\cos\phi_5\right) \quad (28)$$

$$\vec{a}_Q = \left(-S_3\sin\phi_3 + \frac{2}{\beta}S_4\sin\phi_4 - S_5\sin\phi_5 \ , \ S_3\sin\phi_3 - S_5\sin\phi_5\right) \quad (29)$$

$$R_I = -R_3 + \frac{2}{\beta}R_4 - R_5 \quad (30)$$

$$R_Q = R_3 - R_5 = 0\,. \quad (31)$$

The amplitude symmetry condition (10) involves that the terms V_{dcQ}, and R_Q are null. Therefore, the DC component and the rectified wave, $R_Q \cdot n(t)$, will not appear in the regenerated $Q_{out}(t)$ signal. If we consider, in addition to symmetry of ports 3 and 5, that the three outputs are amplitude balanced, that is, $\alpha=1$ and $\beta=1$, the expressions (19) and (20) are reduced to

$$I(t) = \mu_I[-v_3(t) + 2v_4(t) - v_5(t)] \quad (32)$$

$$Q(t) = \mu_Q[v_3(t) - v_5(t)] \quad (33)$$

where

$$\mu_I = \frac{1}{2S_3}\frac{1}{1-\cos(\gamma)} \quad (34)$$

$$\mu_Q = \tan\left(\frac{\gamma}{2}\right)\cdot\mu_I\,. \quad (35)$$

In this case, V_{dcI}, and R_I are null, hence V_{dcI} and $R_I \cdot n(t)$ will be also eliminated in the regenerated $I_{out}(t)$ signal. In any case, the DC components could be eliminated from the recovered I_{out}/Q_{out} signals with analog high-pass filters, or in the digital domain by simply removing the average. On the contrary, the rectified wave, $n(t)$, cannot be eliminated from I_{out}/Q_{out}, as it is a baseband term superposed on the desired signal. The rectified wave increases quadratically with the signal power and, therefore, produces degradation for high power levels.

A. *Orthogonality of the Regenerated I/Q Signals*

$\vec{a}_I$ and $\vec{a}_Q$ form a vector base relating the I/Q signals and the I_{out}/Q_{out} signals. Therefore, the orthogonality of the I_{out}/Q_{out} signals is determined by the vector base orthogonality. This means that the scalar product of $\vec{a}_I$ and $\vec{a}_Q$ must be zero:

$$\vec{a}_I \cdot \vec{a}_Q = \left(-S_3\cos\phi_3 + \frac{2}{\beta}S_4\cos\phi_4 - S_5\cos\phi_5\right)\cdot\left(S_3\cos\phi_3 - S_5\cos\phi_5\right) + \left(-S_3\sin\phi_3 + \frac{2}{\beta}S_4\sin\phi_4 - S_5\sin\phi_5\right)\cdot\left(S_3\sin\phi_3 - S_5\sin\phi_5\right) = 0 \quad (36)$$

Assuming amplitude symmetry in ports 3 and 5 (10), the scalar product results in:

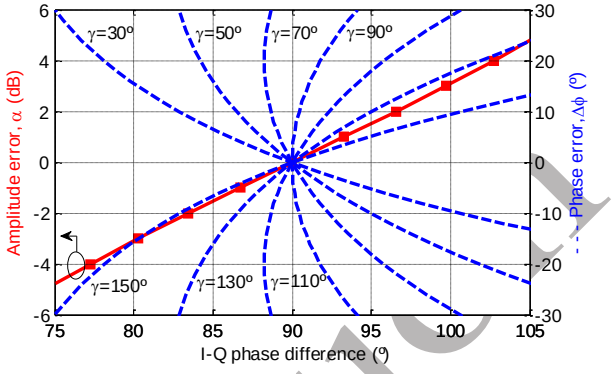

Fig. 3. Orthogonality degradation due to lack of symmetry.

$$\vec{a}_I \cdot \vec{a}_Q = \frac{2}{\beta}S_3S_4\cos(\phi_3 - \phi_4) - \frac{2}{\beta}S_3S_4\cos(\phi_4 - \phi_5)\,, \quad (37)$$

which is equal to zero if:

$$|\phi_3 - \phi_4| = |\phi_4 - \phi_5|\,. \quad (38)$$

This above expression corresponds precisely to the phase symmetry condition (11). Consequently, the orthogonality of the received I_{out}/Q_{out} signals is ensured under the amplitude and phase symmetry conditions expressed in (10)-(11). This means that a symmetrical 3-way RF circuit with respect to port 4 is needed, that is, with symmetry between ports 3 and 5. And most of the five-port circuits in the literature satisfy this condition.

The orthogonality of the regenerated IQ signals does not depend on the value of γ, provided that the amplitude and phase symmetry conditions are fulfilled. Nonetheless, when the five-port circuit response deviates from the symmetrical behavior, the selection of γ can be important. To illustrate this situation, we have simulated the orthogonality degradation due to lack of symmetry. The degradation coming from lack of phase symmetry has been evaluated by introducing a phase error into port 5, that is: $\Phi_3=\gamma$, $\Phi_4=C_0=0$, $\Phi_5=-\gamma-\Delta\Phi$, where $\Delta\Phi$ represents the phase deviation from symmetry. To evaluate the degradation due to lack of amplitude, $v_5(t)$ has been divided by a factor α, which represents the amplitude error. The results are plotted in Fig. 3. The conclusion is that the orthogonality is more vulnerable to phase errors as γ separates from 90º. For example, a ±10º phase error leads to a maximum IQ phase imbalance of 5º for γ=50º and γ=130º; 2.3º for γ=70º and γ=110º; and 0.5º for γ=90º. Moreover, a ±10º IQ phase imbalance can be obtained with amplitude errors of ±3 dB.

B. *Amplitude of the Regenerated I/Q Signals*

The regenerated $I_{out}(t)$ and $Q_{out}(t)$ signals differ from the original I(t) and Q(t) signals by the factors $1/\mu_I$ and $1/\mu_Q$ (25)-(26), respectively. Moreover, μ_I and μ_Q depend on γ as for (34)-(35). This means that, although the selection of γ does not have influence in the fulfillment of condition (11) and,

therefore, in the I_{out}/Q_{out} orthogonality, the amplitude of the regenerated $I_{out}(t)$ and $Q_{out}(t)$ signals will be different

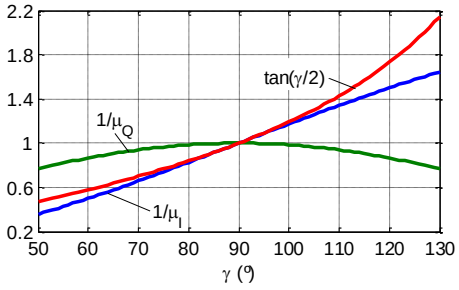

Fig. 4. Variation of $1/\mu_I$, $1/\mu_Q$, and $\tan(\gamma/2)$ with γ

depending on γ.

Let us consider, for simplicity, a fully symmetrical five-port circuit, that is, $\alpha=1$ and $\beta=1$. As it can be derived from (35), the relation between the amplitudes of $I_{out}(t)$ and $Q_{out}(t)$ responds to $\mu_Q/\mu_I=\tan(\gamma/2)$. Therefore, the I-Q amplitude imbalance will be determined by $\tan(\gamma/2)$. Fig. 4 represents the values of $1/\mu_I$, $1/\mu_Q$, and $\tan(\gamma/2)$ as a function of γ, considering the typical value of $S_3=0.5$. As it can be seen, the original I/Q signals can be directly recovered from $I_{out}(t)$ and $Q_{out}(t)$ if $\gamma=90º$, and no amplitude imbalance is observed in this case. The amplitude imbalance increases as γ separates from 90º, so either analog or digital amplitude imbalance correction is required. Around $\gamma=90º$, $1/\mu_Q$ keeps a constant value of 1, and $1/\mu_I$ is equal to $\tan(\gamma/2)$, which presents a linear tendency. An analog amplitude compensation could be easily performed by means of a variable gain block in the I-channel, as the correction can be directly obtained from the received $Q_{out}(t)$ signal. Amplitude imbalance can be also digitally compensated.

The work presented in [17] responds to the particular situation of a five-port circuit with $\gamma=90º$, and the same amplitude response in the three ports. The authors extract the equations describing the I/Q regeneration circuit behavior from these specific conditions, but they do not consider a general five-port junction. However, the design criterion of an optimal five-port network imposes $\gamma=120º$. We have demonstrated that the proposed I/Q regeneration technique can be extended to any five-port structure, as long as it fulfills the amplitude and phase symmetry conditions just in ports 3 and 5 (10)-(11).

C. DC-offset and IMD2 suppression

The quadratic response of the detectors represents a second-order nonlinearity, which generates undesired baseband beats affecting the performance of direct conversion receivers [1],[19]. These undesired distortion terms are represented as $V_{dc,i}$ and $R_i \cdot n(t)$ in (3). Moreover, in the presence of strong interfering signals, other undesirable distortion products can be generated. This situation occurs, for example, when an adjacent channel is located within the bandwidth of the receiver's RF filter. In this case, the RF input signal would be:

$$v_{RF}(t)=\Re e\left\{\left[I(t)+jQ(t)\right]\cdot e^{j2\pi f_{RF}t}+z_{adj}(t)\cdot e^{j2\pi f_{adj}t}\right\},(39)$$

where f_{adj} and $z_{adj}(t)=I_{adj}(t)+jQ_{adj}(t)$ represent, respectively, the frequency and the complex envelope of the adjacent channel signals. If $|f_{adj}-f_{LO}|$ is greater than the cutoff frequency of the low pass filter, the output $v_i(t)$ signals will be:

$$v_i(t)=\frac{K_{2i}}{2}A_i^2V_{LO}^2+\frac{K_{2i}}{2}\left[B_i^2\left(I^2(t)+Q^2(t)\right)+B_{f_{adj},i}^2\left(I_{adj}^2(t)+Q_{adj}^2(t)\right)\right],(40)$$
$$+S_i\left[I(t)\cos(\phi_i)+Q(t)\sin(\phi_i)\right]$$

with $B_{fadj,i}$ the five-port circuit attenuation from the RF port at f_{adj}. Therefore, not only the self-mixing of the LO and useful signals will appear, but also the self-mixing of the adjacent channels, which occupy twice the bandwidth of $I_{adj}(t)$ or $Q_{adj}(t)$. Proceeding as in Section II, (40) can rewritten as follows

$$v_i(t)=V_{dc,i}+dc_i'+R_in(t)+R'_in_{adj}(t)+S_i\left[\cos\phi_iI(t)+\sin\phi_iQ(t)\right],(41)$$

where $R'_i=\frac{K_{2i}}{2}B_{f_{adj},i}^2$. dc_i' and $n_{adj}(t)$ are, respectively, the DC and time variant components of the self-mixing of the adjacent channel. Now the expression of I_{out}/Q_{out} will be:

$$\begin{bmatrix}I_{out}(t)\\Q_{out}(t)\end{bmatrix}=\begin{bmatrix}\vec{a}_I\\\vec{a}_Q\end{bmatrix}\cdot\begin{bmatrix}I(t)\\Q(t)\end{bmatrix}+\begin{bmatrix}R_I\\R_Q\end{bmatrix}\cdot n(t)+\begin{bmatrix}R'_I\\R'_Q\end{bmatrix}\cdot n_{adj}(t)+\begin{bmatrix}V_{dcI}\\V_{dcQ}\end{bmatrix},(42)$$

where $R'_I=-R'_3+\frac{2}{\beta}R'_4-R'_5$, and $R'_Q=R'_3-R'_5=0$.

On one hand, the amplitude symmetry condition between ports 3 and 5 involves that the terms V_{dcQ}, R_Q and R'_Q are null. Hence, no DC-offset and IMD2 will appear in the Q-path. On the other hand, if the same amplitude response is presented in port 4, V_{dcI}, R_I and R'_I will be null, and the DC-offset and IMD2 terms will be also eliminated in the I-path.

Another possible situation that results in the generation of undesirable baseband components is the following. Consider two strong signals, $\cos(2\pi f_1t)$ and $\cos(2\pi f_2t)$, separated in frequency an amount $f_2-f_1=\Delta$, less than the bandwidth of interest. When these signals are exposed to a second-order nonlinear behavior, a baseband beat is generated at Δ Hz:

$$v_i(t)=V_{dc,i}+R_in(t)+\sum_{n=1}^{2}R'_{i,n}n_{adj,n}(t)$$
$$+S_i\left[\cos\phi_iI(t)+\sin\phi_iQ(t)\right]+S'_i\cos(2\pi\Delta t)\quad,\qquad(43)$$

where $S'_i=K_{2i}\cdot B_{f1,i}\cdot B_{f2,i}$, and B_{f1} and B_{f2} are the five-port circuit attenuations from the RF port at frequencies f_1 and f_2. The same conclusions can be extracted in this case: the amplitude symmetry condition between ports 3 and 5 ensures distortion rejection in the Q-signal; considering the same attenuation in port 4, the distortion can be also eliminated in the I-path. Consequently, the IMD2 and the DC-offset can be eliminated in the regenerated I/Q signals if there is the same attenuation in three output ports.

IV. Description of the Prototype

A five-port receiver prototype has been developed in order to validate the proposed I/Q regeneration method. The block diagram of the fabricated five-port receiver is shown in Fig. 5. It is composed of a five-port demodulator circuit and an analog I/Q regeneration circuit. The detailed description of the five-port and I/Q-regeneration circuits is presented bellow.

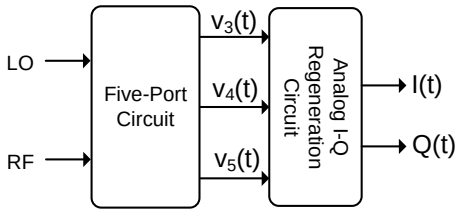

Fig. 5. Block diagram of the developed five-port receiver

A. Five-Port Circuit

Fig. 6 illustrates a photograph of the fabricated five-port circuit, using MIC (Microwave Integrated Circuits) technology. It is composed of a five-port junction and three power detectors. The five-port interferometer is a microstrip ring designed for a 2.1 GHz central frequency, using a FR4 substrate (ε_r=4.7, h=1.59 mm). The power detectors are implemented using the Agilent HSMS2850 Schottky diode.

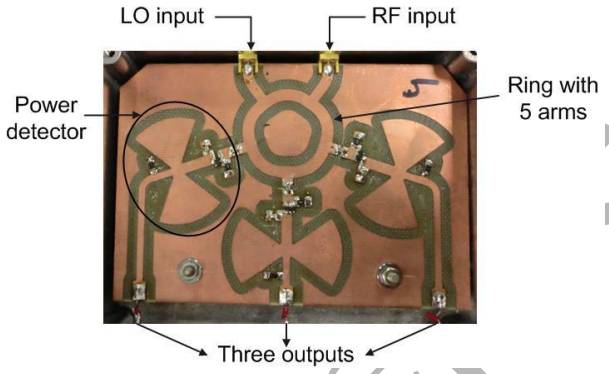

Fig. 6. Fabricated five-port circuit

B. Analog I/Q Regeneration Circuit

Fig. 7 shows the fabricated I/Q regeneration circuit, which responds to the configuration represented in Fig. 2, with $\beta=1$. The values of R1 and R2 have been selected to achieve a voltage gain of 30. Therefore, in order to ensure equal and high load impedance at the three detectors outputs, a simple circuit composed of three followers has been added before the I/Q regeneration circuit.

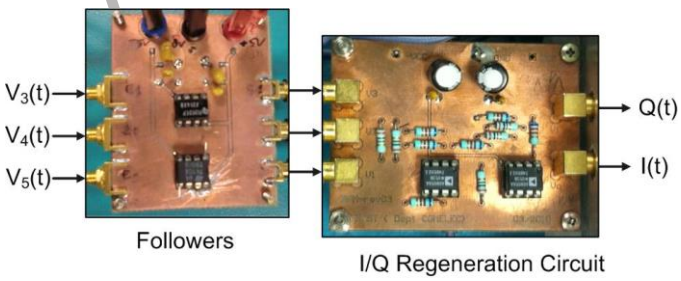

Fig. 7. Fabricated I/Q regeneration circuit

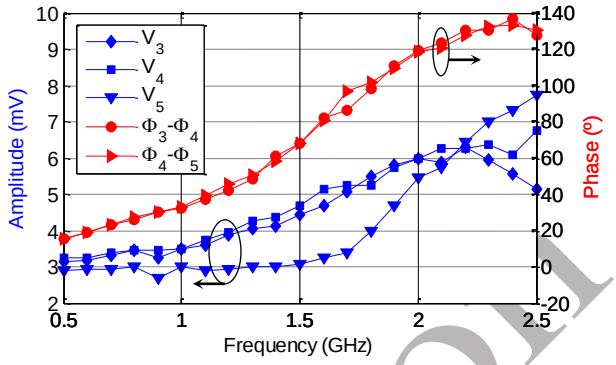

Fig. 8. Measured amplitude and phase shift of the five-port circuit output signals, P_{RF}=-35 dBm, P_{LO}=0 dBm, Δf= 10 KHz.

V. Measurement Results

This section presents the experimental validation of the proposed I/Q regeneration method, as well as the demodulation capacity of the developed five-port receiver.

A. I-Q Phase and Amplitude Imbalance

According to the theory presented in Section III.A, the orthogonality of the regenerated I/Q signals is ensured when both amplitude and phase symmetry conditions (10)-(11) are maintained. Consequently, the first step is to verify if the developed five-port circuit fulfils these symmetry conditions.

Two sinusoidal signals with a 10 kHz frequency displacement are introduced into the RF and LO input ports. These signals come from two Agilent E8267D signal generators, which have been phase locked. The LO power level is fixed to P_{LO}=0 dBm, and the RF power to P_{RF}= -35 dBm. The three output signals of the five-port circuit are introduced into the Agilent 54622A oscilloscope. Fig. 8 represents the measured amplitudes of the three output signals (V_3, V_4, V_5), and the measured phase shifts of signals $v_3(t)$ and $v_5(t)$ with respect to signal $v_4(t)$ (Φ_3-Φ_4, Φ_4-Φ_5). As it can be seen, the circuit keeps phase symmetry in a very large frequency range, from 0.5 to 2.5 GHz. However, the amplitude balance between ports 3 and 5 is only maintained around the central frequency, 2.1 GHz, as five-port rings typically cover less than 20% bandwidth. A ±3.5 dB amplitude imbalance between ports 3 and 5 is observed from 0.5 to 2.5 GHz. Therefore, from Fig. 3, a maximum IQ phase imbalance of 11.5º is foreseen.

Next, the I/Q regeneration circuit is connected to the five-port circuit, and the received I/Q signals are introduced into the Agilent 54622A oscilloscope. The measured amplitudes and phase difference of the received I/Q signals are presented in Fig. 9. The simulated IQ phase imbalance, calculated from the measured five-port circuit response (Fig. 8), is also plotted in Fig. 9. On one hand, a constant phase difference around 90º is maintained from 0.5 to 2.3 GHz, although there is not amplitude symmetry in this frequency range. The maximum phase imbalance is 10º. Consequently, the proposed technique permits to increase the operating frequency of the five-port demodulator. On the other hand, as it was demonstrated in

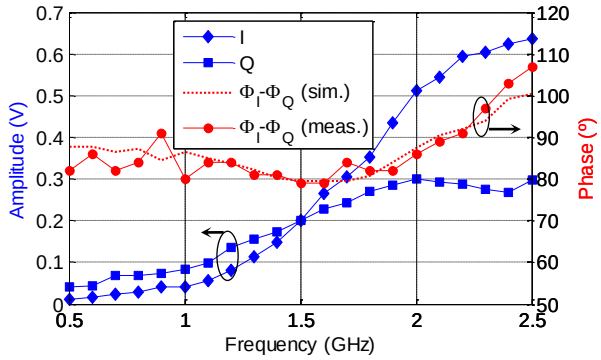

Fig. 9. Measured amplitude and phase of the received I/Q signals, (P_{RF}=-35 dBm, P_{LO}=0 dBm, Δf= 10 KHz), and simulated IQ phase difference.

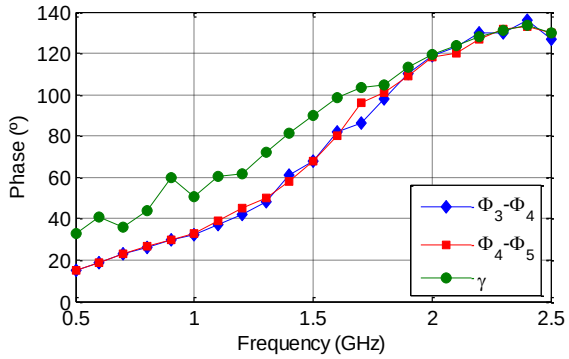

Fig. 10. Comparison between the measured phase shift of the five-port circuit output signals and the value of γ calculated from the measured IQ amplitudes.

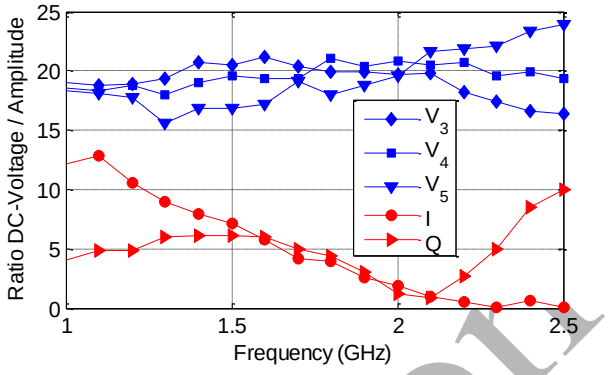

Fig. 11. DC-offset suppression performance versus frequency, P_{LO}=0 dBm.

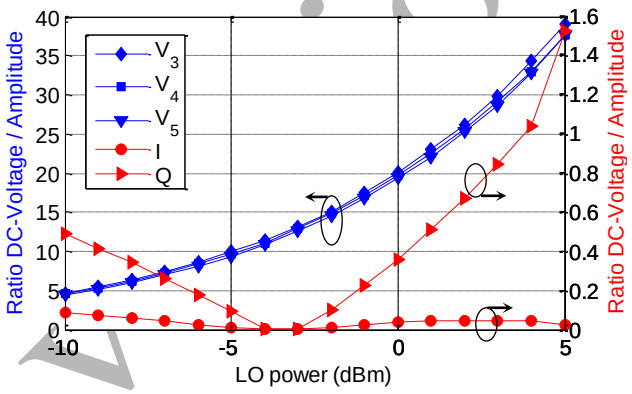

Fig. 12. DC-offset suppression performance versus LO power, f=2.1 GHz.

Section III.B, the relation between the amplitudes of the regenerated I/Q signals is given by the term tan(γ/2). Therefore, the value of γ can be calculated from the measured I/Q amplitudes. The comparison between the calculated value of γ and the measured phase shift of the five-port circuit output signals is presented in Fig. 10. The system follows the theoretical behavior from 1.8 GHz to 2.5 GHz, although there is not perfect amplitude symmetry between ports 3 and 5 (Fig. 8).

B. DC-offset and IMD2 suppression

As it was demonstrated in Section III.C, the IMD2 and the DC-offset can be eliminated in the received I/Q signals if there is the same attenuation in three output ports. The first experiment to prove this affirmation will be carried out without the presence of adjacent channel signals, in order to evaluate just the DC-offset suppression performance. Two sinusoidal signals, coming from two Agilent E8267D generators and separated 10 kHz in frequency, are introduced into the RF and LO input ports. The RF power is P_{RF}=-35 dBm. Since the I/Q regeneration circuit has a voltage gain of 30, the relation between the DC-voltage and the amplitude of the received signal will be evaluated. This relation will be firstly measured at the three five-port circuit outputs, using the Agilent 54622A oscilloscope. It corresponds to the case of using a typical five-port receiver configuration, where the three outputs are directly digitalized. After, we will connect the analog I/Q regeneration circuit between the five-port circuit and the oscilloscope, and the relation will be measured at the I and Q outputs. Setting the LO power to P_{LO}=0 dBm and varying the frequency, the measured results are presented in Fig. 11. Effectively, the ratio DC-voltage/Amplitude is lower in the I/Q signals for all the measured frequency range. This ratio approximates to zero around the central frequency of the five-port circuit, since there is amplitude symmetry and the DC-voltage tends to be null. Fig. 12 shows the ratios DC-voltage/Amplitude as a function of the LO power, fixing a frequency of 2.1 GHz. Once again, the ratio is lower in the I/Q signals for all the values of P_{LO}. In addition, the DC-offset is completely cancelled for values of P_{LO} around -4 and -3 dBm.

Secondly, the IMD2 suppression performance will be evaluated in the presence of strong interfering signals. We have considered the two situations expounded in Section III.C: one interfering adjacent channel signal, and two interfering signals.

In the first situation, both wanted and interfering signals are 100 kbps QPSK modulated signals, located at f_{RF}=2.1 GHz and f_{adj}=2 GHz, respectively. The LO power is P_{LO}=-3 dBm, and the wanted signal power is PRF=-39.8 dBm. The interference power (P_{adj}) will be swept from -30 to 10 dBm. First, we introduce the wanted signal into the input of the five-port circuit. Using a spectrum analyzer, we measure the power concentrated into the baseband signal bandwidth (0-50 kHz), which will be called useful signal power (P_{US}). This power comprises the contribution of the desired signal, and its self-mixing. Next, we introduce the interfering signal and repeat the same measurement. In this case, the measured power corresponds to the self-mixing of the interfering signal

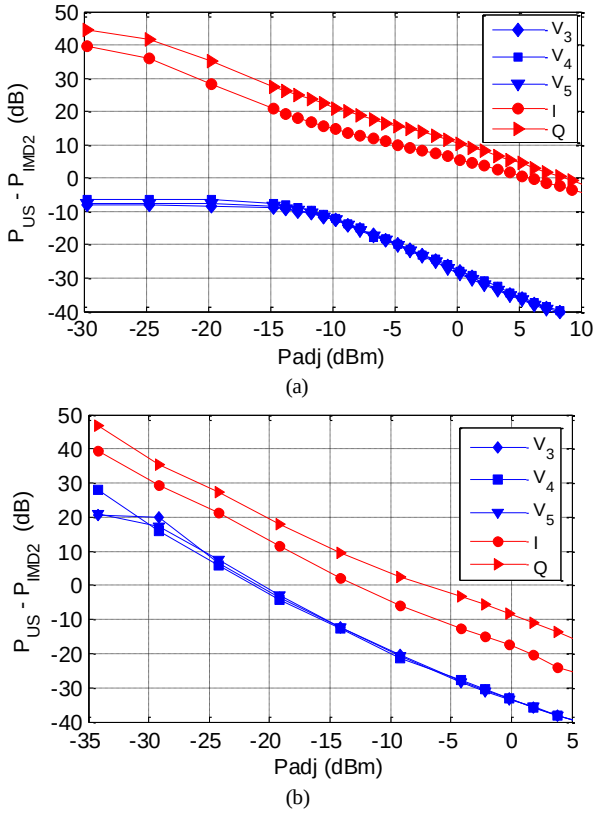

Fig. 13. IMD2 suppression performance versus adjacent channel power, P_{adj} (a) One interfering adjacent channel signal (b) Two interfering signals.

(P_{IMD2}). The measured relation between P_{US} and P_{IMD2} for different values of P_{adj} is shown in Fig. 13 (a). The quadratic behavior of the self-mixing terms can be clearly appreciated in the curves corresponding to V_i. The IMD2 reject improvement with respect to a conventional five-port receiver is evident. P_{US} is lower than P_{IMD2} at the five-port circuit outputs, while the opposite situation happens when the I/Q regeneration circuit is used. The proposed five-port demodulator achieves an increment in the relation P_{US}-P_{IMD2} between 26 and 45 dB.

In the second situation, two tones separated 200 kHz at 2 GHz are combined with the wanted signal, which is a tone separated 10 kHz from the f_{LO}=2.1 GHz. The LO power is P_{LO}=-3 dBm, and the wanted signal power is P_{RF}=-39.8 dBm. Now P_{US} will be the power of the received tone at 10 kHz, and P_{IMD2} will be the power of the interferences beat at 200 kHz. Fig. 13 (b) collects the measured results, where P_{adj} is the power of each interfering tone. In this case, the IMD2 term is linear with the power, as expected from (43). Once again, the improvement in the IMD2 reject is significant, around 15 dB better in the output I, and 23 dB in the output Q.

C. Demodulation results

In this section, we will verify the demodulation capacity of the developed five-port receiver. The test bench is shown in Fig. 14. Two Agilent E8267D signal generators are used as LO and RF QPSK-modulated signals. Both generators are phase locked. The I/Q output signals of the five-port demodulator are sampled by an acquisition card (PCI-6110E National Instruments), using an 800 kHz sampling frequency.

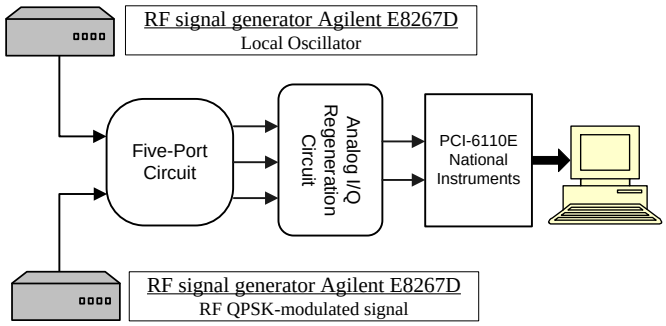

Fig. 14. Test bench.

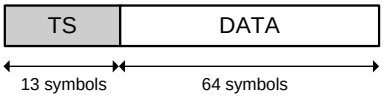

Fig. 15. Structure of the transmitted data burst.

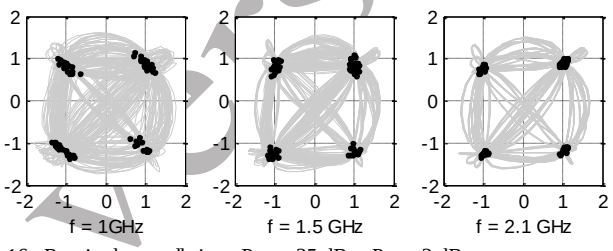

Fig. 16. Received constellations, P_{RF}= -35 dBm, P_{LO}=-3 dBm.

The symbol rate is 100 kbps, thus the over-sampling ratio is OSR=8. The format of the data burst is in conformity with Fig. 15. It consists of a training sequence (TS) and a data sequence. The TS is used to perform the symbol synchronization and the equalization process based on the Minimum Mean Square Error Zero Forcing (MMSE) algorithm, which compensates the amplitude imbalance of the regenerated I/Q signals. The TS is composed of 13 symbols, which correspond to the 26 bits of the GSM TSC1 training sequence. The data sequence is made up of 64 symbols (128 bits).

Fig. 16 shows an example of the QPSK constellation diagrams recovered by our circuit at 1 GHz, 1.5 GHz, and 2 GHz. The represented constellations include all the acquired data (grey traces), and the recovered symbols after synchronization (black points). We observe correct equalization performance, since constellation diagrams are normalized and centered. In addition, the symbol synchronization is good, as the recovered symbols are located close to their ideal position. The variation of the Error Vector Magnitude (EVM) with frequency is also presented in Fig. 17. The value of EVM is quite high, due to the slight rotation that can be observed in the constellations. This rotation comes from the difference between the real behavior of the circuits, and the theoretical I/Q regeneration equations. However, it can be easily compensated in the digital domain. Furthermore, an EVM of 14 % is enough to demodulate a QPSK signal without errors. In any case, the importance of these results is that they demonstrate the demodulation capacity of the system in a large frequency range, even if not perfect five-port symmetry is

achieved.

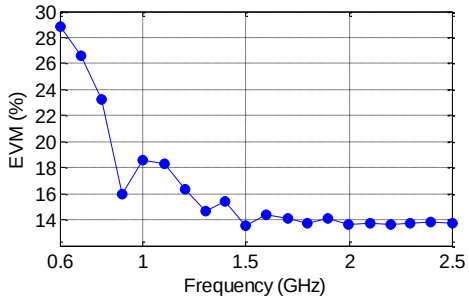

Fig. 17. Measured EVM versus frequency, P_{LO}= -3 dBm, P_{RF}=-35 dBm.

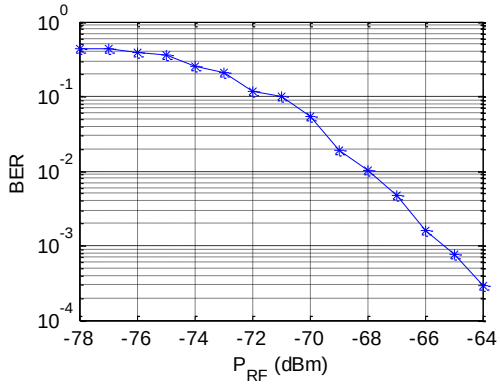

Fig. 18. Measured BER versus RF power of the QPSK modulated signal, f= 2.1 GHz, P_{LO}=-3 dBm.

Finally, we have measured the sensitivity of our receiver, defined as the RF input power to ensure a BER of 10^{-3}. The following figure represents the BER versus the power of QPSK modulated signal. We obtain a sensitivity of –65.4 dBm for the developed five port receiver, without using a low noise amplifier. The sensitivity improves around 3 dB with respect to digital I/Q regeneration [7], as a consequence of the DC-offset cancelation. Furthermore, a BER improvement will be also observed when handing high power levels, or in the presence of interfering signals, due to the IMD2 suppression.

VI. Conclusion

This paper presents a direct baseband I/Q regeneration method applicable to five-port architectures. It is based on the property that the five-port circuit has an axis of symmetry, which can be easily satisfied by five-port and three-phase circuits. The validity of the method has been satisfactorily proved in an experimental five-port receiver. The proposed method overcomes some typical drawbacks of five-port receivers. On one hand, it eliminates one baseband output and the calibration algorithm without any reduction in the operating frequency band. On the other hand, it improves the DC-offset and IMD2 rejection, which are main problems in direct conversion architectures.

References

[1] B. Razavi, "Design considerations for direct-conversion receivers," *IEEE Trans. Circuits Syst.*, vol. 44, no. 6, pp. 428–435, Jun. 1997.

[2] C. de la Morena–Álvarez–Palencia, M. Burgos–García, D. Rodríguez–Aparicio, "Software defined radio technologies for emergency and professional wide band communications," in *IEEE Int. Carnahan Conf. Security Tech.*, San Jose, CA, 2010, pp. 357–363.

[3] J. Crols, M.S.J. Steyaert, "Low-IF topologies for high-performance analog front ends of fully integrated receivers", *IEEE Trans. Circuits Syst. II, Analog Digit. Signal Process.*, vol.45, no.3, pp.269-282, Mar. 1998.

[4] G.F. Engen, "The six-port reflectometer an alternative network analyzer," *IEEE Trans. Microwave Theory Tech.*, vol. 25, pp. 1075–1079, Dec. 1977.

[5] T. Hentschel, "The six-port as a communications receiver," *IEEE Trans. Microw. Theory Tech.*, vol.53, no.3, pp. 1039-1047, March 2005.

[6] C. de la Morena-Álvarez-Palencia, M. Burgos, "Four-octave six-port receiver and its calibration for boradband Communications and software defined radios," *Progress in Electromagnetics Research*, vol. 116, pp. 1-21, April 2011.

[7] G. Neveux, B. Huyart, G.J. Rodriguez-Guisantes, "Wide-band RF receiver using the "five-port" technology," *IEEE Trans. Vehicular Technology*, vol.53, no.5, pp. 1441-1451, Sept. 2004.

[8] K. Mabrouk, F. Rangel, B. Huyart, G. Neveux, "Architectural solution for second-order intermodulation intercept point improvement in direct down-conversion receivers", *IET Microw. Antennas Propag*, vol. 4, no 9, pp. 1377-1386, 2010.

[9] C. Mohamed, A. Khy, B. Huyart, "A (1-20 GHz broadband MMIC demodulator for low-IF receivers in multi-standard applications", *IEEE Microwave Theory and Techniques*, vol. 57, n° 1, pp. 2318-2328, 2009.

[10] S.O. Tatu, E. Moldovan, K. Wu, R.G. Bosisio, "A new direct millimeter-wave six-port receiver," *IEEE Trans. Microwave Theory Tech.*, vol. 49, no.12, pp.2517-2522, Dec. 2001.

[11] J. Östh, A. Serban, Owais, M. Karlsson, S. Gong, J. Haartsen, P. Karlsson, "Six–port gigabit demodulator", *IEEE Trans. Microwave* Theory Tech., Vol. 59, no. 1, pp. 125–131, Jan. 2010.

[12] A. Koelpin, G. Vinci, B. Laemmle, D. Kissinger, R. Weigel: "The six–port in modern society," *IEEE Microw. Magazine*, vol. 11, no. 7, pp. 35–43, Dec. 2010.

[13] C.-H. Wang, H.-Y. Chang, P.-S. Wu, K.-Y. Lin, T.-W. Huang, H. Wang, C. H. Chen, "A 60 GHz low-power six-port transceiver for gigabit software-defined transceiver applications," in *IEEE Int. Solid-State Circuits Conf.*, 11–15 Feb. 2007, pp. 192–596.

[14] Y. Xu, R.G. Bosisio, "Four-port digital millimetric receiver (FP/DMR)", *Microwave Opt. Tech. Lett.*, vol. 22, pp. 350–354, Sept. 1999.

[15] K. Haddadi, H. El Aabbaoui, C. Loyez, D. Glay, N. Rolland, T. Lasri, 'Wide-band 0.9 GHz to 4 GHz four-port receiver', in *IEEE Int. Conf. Electron. Circuits Syst.*, Nice, France, Dec. 2006, pp. 1316–1319.

[16] K. Mabrouk, B. Huyart, "Circuit analogique pour le calibrage large bande, la suppression des tensions parasites dues aux DC-offset et produits d'intermodulation IMD2 et réduction d'un convertisseur CAN pour les démodulateurs Zéro-IF ou Low-IF de type cinq-port et triphasé", Patent FR2934934 (A1) - 2010-02-12.

[17] R. Mirzavand, A. Mohammadi, A. Abdipour, "Low-cost implementation of broadband microwave receivers in Ka-band using multiport structures," *IET Microw. Antennas Propag.*, vol. 3, no. 3, pp. 483-491, 2009.

[18] M. Mohajer, A. Mohammadi, A. Abdipour, "Direct conversion receivers using multiport structures for software-defined radio systems," IET Microwaves, Antennas & Propagation, vol. 1, no. 2, pp. 363–372, 2007.

[19] E.E. Bautista, B. Bastani, J. Heck, "A high IIP2 downconversion mixer using dynamic matching," *IEEE J. Solid-State Circuits*, vol.35, no.12, pp.1934-1941, Dec 2000.

Cristina de la Morena-Álvarez-Palencia was born in Toledo, Spain, in 1982. She received the Telecommunication Engineering degree from the Universidad Politécnica de Madrid (UPM), Madrid, Spain, in 2007. She is currently working towards the PhD degree at UPM. Since April 2006, she has been with the Microwave and Radar Group, Department of Signals, Systems and Radiocommunications (SSR), UPM. Her research activities include high-frequency

and microwave circuit design, with special interest in six-port reflectometers using hybrid technology and Low Temperature Co-fired Ceramic (LTCC). She is also involved in radio frequency subsystems and broadband digital receivers for advanced applications and Software Defined Radios.

Kaïs Mabrouk (S'08) was born in Montereau Fault-Yonne, France, in 1979. He received the B.S. degree in electrical and electronics engineering from the Tunis College of Sciences and Techniques, Tunis, Tunisia, in 2003, the Master degree in telecommunications engineering from the Pierre et Marie Curie University, Paris, France, in 2004, and the Ph.D. degree at the École Nationale Supérieure des Télécommunications (ENST)–TELECOM ParisTech, Paris, France in 2008. After an industrial experience at SAGEM Mobile, he joined ESIGETEL in 2010 and he found ALTRONIC group. At ESIGETEL he manages a research group (Loc'In) on Indoor Localization using wireless Technologies and he continues its research activities with Telecom ParisTech on transceiver design for telecommunications applications and multiple antenna systems.

Bernard Huyart received the Electrical Engineer degree from the University of Lille (Polytech'Lille), France, in 1977, and the Doctoral degree in physics from the Ecole Nationale Supérieure des Télécommunications (ENST), Paris, France, in 1986. In 1995, he earned the accreditation to supervise research from the University of Limoges, France. In 1978, he joined Telecom ParisTech, where he is currently a Full Professor and Head of the Radiofrequencies and Microwaves Group, which is associated with the Centre National de la Recherche Scientifique (CNRS) [Unité Mixte de Recherche (UMR) 5141]. His current research interests include microwave instrumentation, the design of mixers and six-port reflectometers in microwave monolithic integrated circuit (MMIC) or hybrid technology, noise and nonlinear devices measurement and modelization, and the applications of six-port techniques in telecommunications (estimation of direction-of-arrival (DOA) of RF signals and direct demodulation) and in radar systems.

Amadou Mbaye was in born in Dakar, Senegal, in 1987. He received the Networks and Telecommunications Engineering degree From Ecole Nationale Supérieure de l'Electronique et de ses Applications (ENSEA), Cergy, France in 2011. During his last internship as engineer student, he worked on Spectrum Aggregation by means of the Tri-Phase Demodulator and the I/Q regeneration circuit presented in this paper. Now he is looking for a PhD on signal processing for communication systems.

Mateo Burgos-García received the Ingeniero de Telecomunicación and Ph. D. degrees from the Universidad Politécnica de Madrid (UPM), Madrid, Spain, in 1989 and 1994, respectively. Since September 1988, he has been with the Grupo de Microondas y Radar, Departamento de Señales, Sistemas y Radiocomunicaciones, UPM, where he is full professor. His research activities include broadband digital receivers for spectrum surveillance and software defined radios, broadband radars for low probability of interception (LPI) and high resolution applications, millimeter-wave radars and synthetic aperture radar (SAR) signal processing.